Stereo Vision Based Automated Solder Ball Height Detection

Jinjin Li[1], Bonnie L. Bennett[2], Lina J. Karam[1], and Jeff S. Pettinato[2]
[1]School of Electrical, Computer, & Energy Engineering, Arizona State University, Tempe, AZ, USA
[2]Intel Corporation, USA

Abstract

Solder ball height inspection is essential to the detection of potential connectivity issues in semi-conductor units. Current ball height inspection tools such as laser profiling, fringe projection and confocal microscopy are expensive, require complicated setup and are slow, which makes them difficult to use in a real-time manufacturing setting. Therefore, a reliable, in-line ball height measurement method is needed for inspecting units undergoing assembly.

Existing stereo vision measurement techniques determine the height of objects by detecting corresponding feature points in two views of the same scene taken from different viewpoints. After detecting the matching feature points, triangulation methods are used to determine the height or depth of an object. The issue with existing techniques is that they rely on the presence of edges, corners and surface texture for the detection of feature points. Therefore, these techniques cannot be directly applied to the measurement of solder ball height due to the textureless, edgeless, smooth surfaces of solder balls.

In this paper, an automatic, stereo vision based, in-line ball height inspection method is presented. The proposed method includes an imaging setup together with a computer vision algorithm for reliable, in-line ball height measurement. The imaging set up consists of two different cameras mounted at two opposing angles with ring lighting around each camera lens which allows the capture of two images of a semi-conductor package in parallel. The lighting provides a means to generate features on the balls which are then used to determine height. Determining and grouping points with the same intensity on the ball surface allows the formation of curves, also known as iso-contours, which are then matched between the two views. Finally, an optimized triangulation is performed to determine ball height. The method has been tested on 3 products and exhibits accuracy within 4um mean squared error compared to confocal ground truth height, and the coplanarity of BGA package as derived from calculated substrate depth results.

1. Introduction

Defective solder joints on BGA (Ball Grid Array) can cause problems in semi-conductor products, including non-wets and infant mortality resulting in failed parts. In order to reduce the potential for late detection of warped or defective parts resulting in potential added cost for a defective unit and escapee to a customer, the inspection of solder joints of BGA is an important process in manufacturing. The solder joint bonding ability and reliability is highly dependent on the uniformity of solder ball heights and coplanarity across the unit substrate. Non-uniform solder ball heights can result in non-wets which cause connectivity failures and result in failed units. Warpage can also cause connectivity failures as well as result in infant mortality due to connectivity failures at joints with minimal or weak connectivity. Thus the inspection of solder ball heights is essential in the detection and identification of defects in a timely manner before defective units escape to the customer.

Numerous methods have been developed in recent years for solder ball height measurements. Traditional methods such as visual inspection and in-circuit functional tests are not able to analyze the solder ball layout and height information, and they are usually time-consuming and produce variable results. Nowadays, automated methods are developed to produce more reliable and accurate ball height results. These methods include 3D X-ray laminography [1], laser scanning [2], Moiré projection (Fringe Moiré and shadow Moiré) [3], confocal microscopy [4], shadow graph [5], and machine vision methods [6].

A common factory floor tool for warpage inspection is a model-based method which requires a-priori reference and calibration by a microscope tool tested on several hundred BGA units for each type of product. The sampling and testing procedure of the reference microscope tool is time-consuming. This factory floor tool assumes uniform ball height from the model height, and is not able to compute the absolute ball height for each solder ball. If the incorrect model ball heights are used, there will be mis-detection of warpage and potential for defects and escapees due to incorrect ball size not being detected. The machine vision method in [6] acquire images of the wafer package using two cameras with directional lighting and, for each image, the ball peaks are located by determining the position of the brightest point in each solder ball region, However, the assumption that the ball peaks correspond to highest intensity points is not valid in practice as shown later in this paper. In addition, the method of [6] just calculates the position of the ball peaks with respect to the image origin and not ball peak heights. In addition, the method of [6] assumes that the majority of ball peaks are co-planar, which implies that most of the balls have the same height, and uses this assumption to determine a linear planar transformation (homography) describing the relation between the ball peak positions in the two views. The computed transformation is then applied to the positions of ball peaks in one view. The deviation between the resulting transformed positions and the actual positions in the

second view is computed and used to flag balls with large deviations as defective. Some of the automated ball height detection methods [1][2][3][4][5] are able to provide accurate ball height information, but they usually require high-cost equipment and complicated setup, and the measuring speed is slow. The Moiré projection method [3] projects periodic fringe patterns on the package surface and generates absolute ball height from the deformation of the projected waveforms on the solder ball packages. But the phase unwrapping in the Moiré projection methods produces inaccuracy in the ball height results, and it is computationally intensive and time consuming. The motion control system and integrated workstation of the Moiré projection methods are usually expensive and requires complex training. Another height inspection method [5] calculates absolute ball height from the shadowgraph of balls in the images generated by an oblique collimated light source. But this method is only used on wafers, and might not be usable for solder balls. The collimated light setup requires a number of expensive optical lenses. The size of the whole setup is large and is not suitable for in-line ball height inspection in a manufacturing process. Due to the set up complexity and limited measurement execution speed, existing automated solder ball height measuring methods are not suitable for a real-time ball height inspection process. Therefore, a reliable, fast, in-line ball height measurement method is needed for inspecting units undergoing assembly.

Existing stereo vision measurement techniques determine the height of objects by detecting corresponding feature points in two views of the same scene taken from different viewpoints. The images in stereo matching research are usually taken from a natural scene or manmade objects, which has distinct features for each object in the scene for matching, such as color and gradient. There are various methods proposed for the stereo matching [7][8][9], but a common issue with existing techniques is that they rely on the presence of edges, corners and surface texture for the detection of feature points. Therefore, these techniques cannot be applied to the measurement of solder ball height due to the textureless, edgeless, smooth surfaces of solder balls.

In this paper, an automatic, stereo vision based, in-line ball height inspection method is presented. The method proposed in this paper is computationally efficient compared to other image processing techniques for solder ball height detection. The setup procedure of this method is much simpler than other existing methods' equipment. The imaging set up consists of two different area-scan cameras mounted at two opposing angles with ring lighting around each camera lens which allows the capture of two images of a semi-conductor package in parallel. The computer vision algorithm consists of the calibration of stereo cameras, segmenting individual balls, detecting substrate feature points and ball peak feature points in stereo views, triangulation of corresponding points and calculating ball height. The camera parameters including intrinsic parameters and extrinsic parameters are calculated in the calibration process. The segmentation of each individual ball is achieved using histogram thresholding and a boundary circle-fitting algorithm. The feature points of the substrate are detected using the segmented ball mask, and the feature points of the ball peak are determined by grouping points with the same intensity on the ball surface allows the formation of curves, also known as iso-contours, which are then matched between the two views. Finally, an optimized triangulation is performed to determine feature point depth and ball height, and coplanarity is calculated from the determined substrate depth.

The proposed ball height calculation method was tested on three different types of BGA products, which have different ball sizes, ball surface appearance, ball pitch and layout. The results are compared with the ground truth obtained by an existing confocal inspection tool. The confocal tool is primarily suitable for sampling measurements due to a slower speed and a lengthy calibration process. The error margin of the confocal tool was established to be 7um. The accuracy of the proposed algorithm is within 4um mean squared error compared with the confocal results. The coplanarity of the BGA package is derived from the computed substrate depth results in the proposed algorithm. The results show that the proposed method is capable of calculating the ball height and warpage on BGA packages, and that the produced results are comparable to the results produced by other methods that require expensive equipment and complicated processing software.

This paper is organized as follows. The stereo camera setup and camera calibration process are presented in Section 2. The proposed feature detection algorithm and ball height calculation algorithm are presented in Section 3. The experimental results and performance analysis with existing schemes are presented in Section 4. Conclusions are drawn in Section 5.

2. Imaging Setup and Camera Calibration

The imaging setup in this paper uses two stereo cameras mounted at two opposite angles with a ring light around each camera lens, which allows the capture of two images of a semi-conductor package in parallel. The BGA package is placed on a tray holder under both cameras' field of view. The ring light around each camera generates straight light beams that shine on top of the solder ball surface.
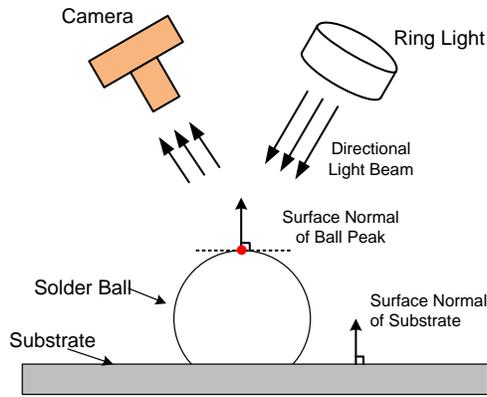
Fig. 1. Illustration of the ball peak point reflection in the imaging setup

The surface of the solder balls is reflective to directional light. It is assumed that, with the previously described setup, the ball peak points on the ball surface that have the same surface normal with that of the substrate surface will reflect the illumination into the camera [6], as illustrated in Fig. 1. Thus these ball peak points will appear bright in the captured images. Other points, whose surface normal vectors have a direction that is different from that of the normal of the substrate surface, will reflect the directional light to other directions that cannot be captured by the CCD camera, and thus appear darker in the captured images. In the stereo images captured by the two cameras at opposite angles, the bright regions near the center of each individual ball contain or surround the ball peak area of solder balls.

In stereo vision algorithms, the internal camera configurations and the relative poses of the stereo cameras are computed through the camera calibration process. The camera parameters consist of intrinsic parameters, such as focal length and principal points, and extrinsic parameters, such as the rotation matrix and translation vectors between stereo cameras. In order to estimate the camera matrices of the stereo cameras, the camera calibration method used in this paper makes use of the Camera Calibration Toolbox [10] [11], which computes the camera parameters from the feature points of a planar calibration pattern in multiple views through a closed-form solution and a minimum mean-squared error (MSE) based nonlinear refinement procedure. The camera calibration is implemented using multiple captured image pairs and a stereo calibration method [11] in order to obtain the camera parameters of the left and right cameras.

3. Proposed Automated Ball Height Inspection Method

In this section, we present more details about the proposed ball height detection algorithm which is capable of calculating accurate solder ball heights on different products. Fig. 2 shows the flowchart of the proposed ball height inspection method. The block diagram summarizes the steps of the proposed method including individual solder ball segmentation and matching, substrate feature point detection, ball peak feature point detection and matching, triangulation and ball height calculation. Fig. 3 illustrates the output results of the main components of the block diagram shown in Fig. 2. More details about the ball segmentation, feature point matching and triangulation are provided in Sections 3.1 to 3.3 below.

3.1 Individual ball segmentation and matching

The accuracy of the matching process of ball feature points is one of the main factors that affect the accuracy of the final height results. In the feature matching process, the first basic step is to match the individual balls in the left view and right view correctly. For this purpose, the individual balls are segmented and labeled in a row-wise order. A ball with the same label number in the left and right views correspond to the same imaged physical ball. The segmentation of BGA images segments out two regions, the balls region and the substrate region. The segmentation method used in this paper consists of an adaptive thresholding method based on histogram analysis [12]. Using the automatic threshold calculation algorithm in [12] and morphological opening operations, the round-shape ball regions for each individual ball can be segmented. The boundary of each individual ball mask is refined using circle fitting. An example of left view and right view images of a solder ball is shown in Fig. 3 (a), and the corresponding segmented ball masks are shown in Fig. 3 (b). In addition, for the same imaged physical ball, the highest intensity region containing or surrounding the ball peak occurs at different locations in the left and right views due to the opposite imaging angles of the left and right cameras, as shown in Fig. 3 (a). Therefore, template matching is performed for each matching pair of solder balls, using the segmented ball in one view as the template, in order to correct for this deviation. The bright region aligned images in the left and right view are shown in Fig. 3 (c). This will enable a more accurate matching of the locations of the corresponding ball peaks as described in Section 3.2.

3.2 Feature Point Detection

After the balls are segmented and matched in the two camera views, ball peak points as well as substrate points need to be localized and matched in the left and right camera views in order to determine the ball heights. In order to measure the ball height, the goal is to find the bottom substrate point and the peak point of each solder ball from the features in the stereo 2D
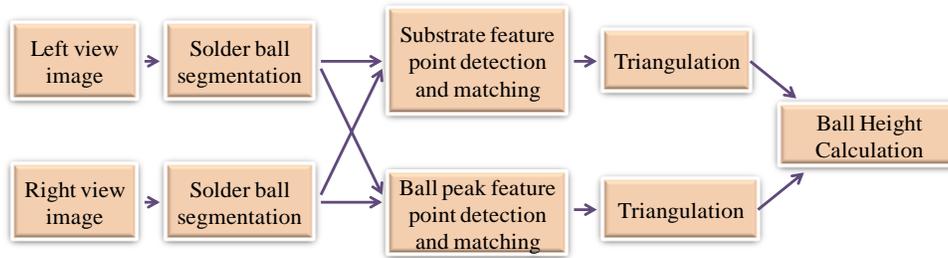

Fig. 2. Block diagram of the proposed solder ball height inspection method

(a). An example of left- and right-view image of a solder ball.

(b). The segmented ball mask of the images shown in (a).

(c). Ball images after bright region alignment with substrate feature points (green) plotted.

(d). zoomed bright regions of left view and right view.

(e). Iso-contour map of the circled regions as shown in (d).

(f). Same color represents matching iso-contour and matching ball peak feature points.

(g) Plotting of 3D ball peak points and substrate point and the corresponding ball heights.

Fig. 3. Steps of the proposed ball height detection method

images. However, the main difficulty in feature detection is that the surfaces of the solder balls are textureless and edgeless, which makes the popular feature detection algorithms, such as the Canny edge detector and the SIFT (Scale Invariant Feature Transform) [13] unsuitable for finding the correct matching features. This is also the main reason why few stereo vision methods are used in the solder ball height inspection area.

The bottom points of each solder ball are the points that lie on the same surface as the substrate of the BGA package. Since the solder balls are placed on the substrate using a paste or fluxing technique, the circle-shape boundary where each individual solder ball touches the substrate can be used to generate the bottom points for each solder ball. In the 2D image captured by the CCD camera, the boundary between a solder ball and the substrate surface is the ball mask boundary of the considered ball. For each individual ball, the centroid of the boundary points represents the imaginary point lying under the solder ball surface on the substrate surface. Thus, for each pair of matching solder balls in the stereo images, the ball mask

boundary and its corresponding centroid are calculated for each ball in the pair. The computed centroid points corresponding to a matched solder ball pair in the left and right views are taken as the matched feature points on the substrate. The 2D corresponding substrate feature points of the ball images in Fig. 3 (a) are plotted as the green star points in Fig. 3 (c).

Compared to the substrate feature point detection, the feature point detection and matching for ball peaks is more complicated. In our proposed method, we exploit the fact that, in the captured pair of images, the ball peaks should belong to or be surrounded by areas of high intensities due to the employed imaging and lighting set-up as described in Section 2. In real-world manufacturing environments, not all solder balls have ideal surfaces; some ball surfaces may be slightly scratched or worn off. Thus the ball surfaces are of different types on the BGA packages. In addition, the imaged surface of a solder ball results in different bright regions in the left and right view due to local variations in the reflective surface characteristics of the solder ball as shown in Fig. 3 (a). Due to the difference in the formed bright regions in the two views and to the variations in the reflective surface characteristics of solder balls, a robust matching algorithm suitable for the different types of solder ball surfaces is needed. In this paper, a novel iso-contour based matching algorithm is applied to detect the matching bright regions between stereo views.

In our proposed method, points with the same intensity are determined on the ball surface and are grouped together to form curves of similar intensities, also known as iso-contours, which are then matched between the two views. In each individual ball region, multiple iso-contours are contained in a bright region intensity range. The lower threshold of the intensity range is determined using the adaptive thresholding method based on histogram analysis [12], and the higher threshold is the highest gray-scale level in the ball region. The iso-contours of various intensities in the bright region are nested from highest intensity to lowest intensity as shown in Fig. 3 (e). For a set of intensities ranging from a minimum value to a maximum value, the nesting relationship of iso-contours can be represented effectively using a tree graph structure, called the inclusion tree structure [14] The tree graph structures are formed for the left and right views and are used to match iso-contours according to the characteristics (centroid distance, area difference, overlap ratio between left- and right-view) of the outermost iso-contour of each bright region. Once the matching pairs of regions (represented by the matching outermost contours) are determined between the left view and right view, for each matching pair, the iso-contours that correspond to or are nested within the outermost contours, those with the largest average intensity gradient magnitude values in each view are chosen as the matching iso-contour curves. For each pair of matching bright regions, the coordinates of the centroid points of the matching iso-contour curves are calculated, and these matching centroid points, one matching centroid pair per region, are used as the matching feature points for the considered ball peak between the left view and right view. An example of the matching iso-contour curves and centroids for multiple matching bright regions are plotted in the ball image shown in Fig. 3 (f). These matching pairs of centroid points are referred to as candidate ball peak feature point pairs and are further used to calculate the ball heights using the triangulation method as discussed in Section 3.3.

3.3 Triangulation and Ball Height Calculation

Once the corresponding feature points of substrate and solder ball peak are located in the stereo images, the triangulation method [15] is used to obtain the 3D reconstruction of these feature points.

As illustrated in Fig. 4, ideally, in the 3D space, the intersection of the two lines, which are formed by connecting each of the matching 2D points and their corresponding camera centers, can be computed to get the corresponding 3D point in space. But due to the presence of noise and digitization errors, it is possible that the intersection of these two rays does not exist in the 3D space. In this paper, a triangulation method that is enhanced using epipolar constraints [15] is adopted and applied in order to localize a pair of corrected 2D feature points $\hat{x}_L$ and $\hat{x}_R$ that ensure the existence of the 3D point in the 3D space. In order to locate the corrected set of 2D matching feature points at the sub-pixel level, the images are interpolated by an integer factor before feature point detection and matching. Using the corrected matching feature points in both views and the calibrated camera projection matrix, the coordinates of the 3D point corresponding to the matched 2D points in the left and right images are computed using linear triangulation based on singular value decomposition (SVD) [16].

For each individual ball, the 3D point of the ball bottom on the substrate and the candidate 3D points of ball peaks, one for each candidate ball peak feature point pair (Section 3.2), are calculated through triangulation. The Euclidean distance between the coordinates of each candidate 3D ball peak point and corresponding 3D ball bottom point is calculated as the ball height value. For a given ball, it is possible to obtain multiple best matching pairs of ball peak regions as described in Section 3.2. In this latter case, for the considered ball, multiple candidate 3D ball peak points and corresponding ball heights are calculated, one for each candidate ball peak feature point pair. For each considered solder ball, the mean and standard deviation of the obtained candidate ball heights are computed and are used to eliminate outlier candidate 3D ball peak points. The 3D ball peak points whose ball height deviates by twice the standard deviation from the mean.are considered as outliers and removed. The highest value in the remaining ball heights is selected as the solder ball height. An example of multiple ball peaks and corresponding ball heights is shown in Fig. 3 (g).

4. Simulation Results

The proposed method was applied to different product lines: A, B and C. Each one of these product lines has different solder ball layout and different ball characteristics. The average ball height for product A, B, C is approximately 280um, 280um and 380um respectively. Example images of solder balls, one from each of the three products, are shown in Fig. 5. The results of the proposed algorithm were compared to the results obtained from the existing automated confocal inspection system.
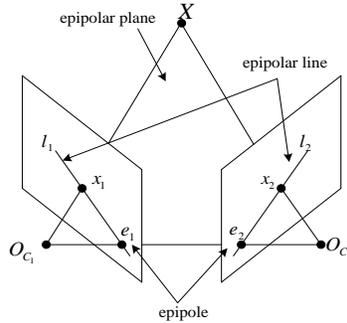

Fig. 4. Epipolar geometry between two views
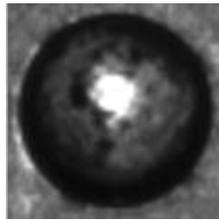
(a) Solder ball of product A. (b) Solder ball of product B. (c) Solder ball of product C.
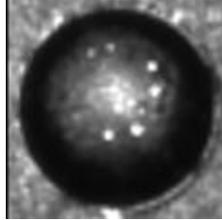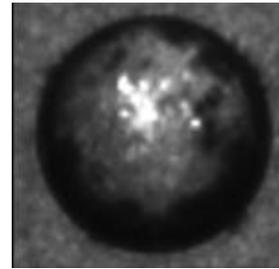
Fig. 5. Examples of solder balls of three BGA products

For the solder balls in one row on the BGA package, the depth value of substrate and ball peak feature points with respect to the left camera are plotted in Fig. 6. Since both cameras are placed over the BGA package, the substrate depth values are larger (greater distance from the camera) than the ball peak depth values (lesser distance from the camera) when viewed from the camera center. The ball height is obtained by calculating the Euclidean distance between the substrate 3D point and the ball peak 3D point. The solder ball height values are plotted in a row-wise order, and compared to the results provided by the confocal tool, as shown in Fig. 6. In this case, the mean squared error compared with confocal ground truth results is 2.03um.

For each product line, a number of packages are randomly selected and imaged using the proposed stereo setup. The statistics of the difference between the calculated ball height results and confocal inspection results are plotted as a bar graph in Fig. 8. From the plotted bar graphs, the results show that the ball height calculated for all three different products are stable and consistent on different packages. The mean square difference compared with the confocal ball height results are within 4 um.

Furthermore, the coplanarity of the BGA package can be represented using the depth of substrate points corresponding to each individual ball. The coordinates of 3D substrate points with respect to the left camera are transformed to 3D points with respect to the BGA package with the origin point taken to be located at the top left corner of the imaged package. In the considered BGA package 3D coordinate system, the depth values of the substrate point represent the coplanarity of the package. The 3D plot of the 3D substrate points over 4 solder ball rows of package are shown in Fig. 9 (a) using the proposed method (blue dot). For comparison, Fig. 9 (a) also shows the 3D substrate points obtained using the confocal tool (red star). Fig. 9 (b) shows the coplanarity of the solder balls in one row as compared to the confocal coplanarity results. As seen in Fig. 9, the depth values of the ball substrate points are following a curved-shape change, which reflects the warpage of the BGA package. The difference in coplanarity measurements between the results obtained using the proposed method and those obtained using the confocal tool is within 9um.

5. Conclusion

A robust automatic solder ball height detection scheme is presented to allow automated inspection and automated measurement of solder ball height. The proposed method is fully automated and can benefit the manufacturing process by measuring ball height and package coplanarity accurately. The proposed method has been implemented in software and was deployed on a standalone PC using the 2D images obtained from a simple imaging setup consisting of two cameras and directional ring lights. The proposed method can accurately and consistently compute solder ball heights. The computed solder ball heights are within a 4um mean squared error range as compared to the results produced by the confocal tool. The proposed method has a low computational complexity and enables real-time in-line ball height and warpage inspection during manufacturing.
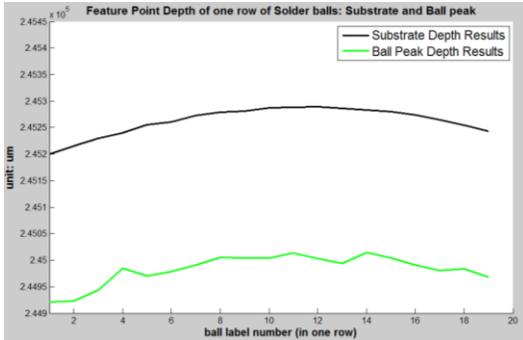
Fig. 6. Calculated ball peak depth and substrate depth with respect to the left camera for one row of solder balls.
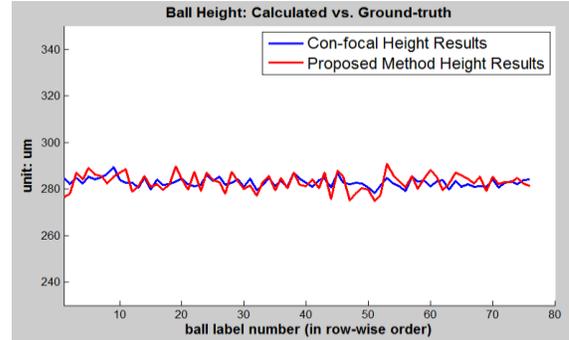
Fig. 7. Calculated solder ball height results compared to confocal ground truth ball height

Fig. 8. MSE of calculated ball height results compared to confocal results for three products.
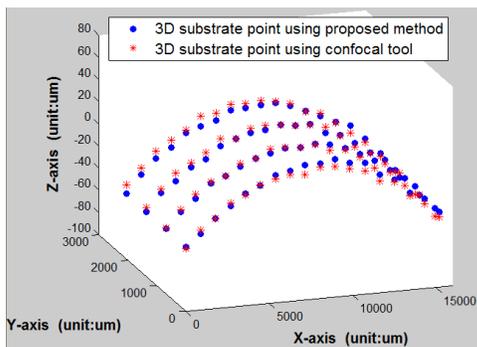
(a). 3D plot of substrate points.   (b) Plot of substrate depth of one row of solder balls. .
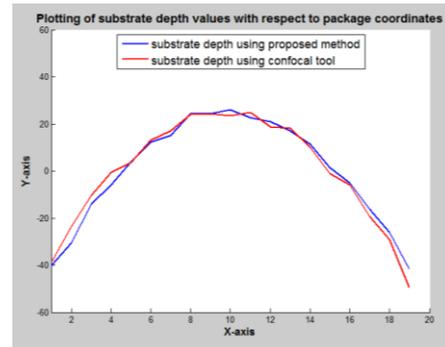
Fig. 9. 3D substrate points with respect to the package top left corner as origin, and coplanarity comparison with confocal results.

References

jinjinli@asu.edu, bonnie.l.bennett@intel.com, karam@asu.edu, jeffrey.s.pettinato@intel.com

[1] A. R. Kalukin and V. Sankaran, "Three_Dimensional Visualization of Multilayered assemblies Using X-Ray Laminography," IEEE Transactions on Components, Packaging, and Manufacturing Technology, Part A, vol. 20, no.3, 1997.

[2] P. Kim and S. Rhee, "Three_Dimensional Inspection of Ball Grid Array Using Laser Vision Stystem," IEEE Transactions on Electronics Packaging Manufacturing, vol. 22, no. 2, 1999.

[3] H. Ding, R. E. Powell, C. R. Hanna and I. C. Ume, "Warpage Measurement Comparison Using Shadow Moiré and Projection Moiré Methods," IEEE Transactions on Components and Packaging Technologies, vol. 25, no. 4, 2002.

[4] G. Udupa, M. Singaperumal, R. S. Sirohi and M. P. Kothiyal, "Characterization of Surface Topography by Confocal Microscopy: I. Principles and the Measurement System," Measurement Science and Technology,vol. 11, no. 3, pp. 305, 2000.

[5] S. Wang, C. Quan and C. J. Tay, "Optical Micro-shadowgraph-based Method for Measuring Micro-solderball Height," Optical Engineering, vol. 44, no. 5, 2005.

[6] M.Dong, R.Chung, Y.Zhao and E.Y. Lam, "Height Inspection of Wafer Bumps Without Explicit 3D Reconstruction," Proceedings of SPIE the International Society for Optical Engineering, vol. 6070, pp. 607004, 2006.

[7] D. Scharstein and R. Szeliski, "A taxonomy and evaluation of dense two-frame stereo correspondence algorithms," International Journal of Computer Vision, vol. 47, no. 7, pp. 42, 2002.

[8] A. Klaus, M. Sormann and K. Karner, "Segment-based Stereo Matching using Belief Propagation and a Self-adapting Dissimilarity Measure," *ICPR*, 2006.

[9] Z. Wang and Z. Zheng, "A Region Based Stereo Matching Algorithm using Cooperative Optimization," *CVPR*, 2008.

[10] Z. Zhang, "Flexible Camera Calibration by Viewing a Plane From Unknown Orientations," The Proceedings of the 7th IEEE International Conference on Computer Vision, vol. 1, pp. 666-673, 1999.

[11] Camera Calibration Toolbox for Matlab Website: http://www.vision.caltech.edu/bouguetj/calib_doc/index.html#ref

[12] A. F. Said, B. L. Bennett, L. J. Karam and J. S. Pettinato, "Automated Detection and Classification of Non-wet Solder Joints," IEEE Transactions on Automation Science and Engineering, vol. 8, no. 1, 2011.

[13] D. Lowe, "Distinctive Image Features from Scale-Invariant Keypoints," International Journal of Computer Vision, vol. 60, no. 2, pp. 91–110, 2004.

[14] B. Hong and M. Brady, "A Topographic Representation for Mammogram Segmentation," Medical Image Computing and Computer-Assisted Intervention, vol. 2879, pp. 730-737, 2003.

[15] R. Hartley and A. Zisserman, "Multiple View Geometry in Computer Vision," Cambridge University Press, 2002.

[16] G. H. Golub and C. Reinsch, "Singular Value Decomposition and Least Squares Solutions," Numerische Mathmatik, vol. 14, no. 5, pp 403-420, 1970.

Stereo Vision Based Automated Solder Ball Height Detection

Bonnie Bennett and Jeff Pettinato
Intel Corporation
Jinjin Li and Dr. Lina Karam
Arizona State University

Agenda

- Problem Statement and introduction
- Imaging Setup and Camera Calibration
- Automated Solder Ball Height Detection Method
- Experimental Results (Ball Height and Warpage)
- Summary

Problem Statement

- Defective solder joints on BGA can cause problems in semi-conductor products, including non-wets and infant mortality resulting in failed parts

- The inspection of solder ball heights is essential in the detection and identification of defects in a timely manner before defective units escape to the customer

Limitations – Existing Solder Ball Height Detection Methods

Methods	Pros	Cons
Factory tool	Real-time processing	Relies on sampling testing. No absolute height. Assumes uniform height.
Homography method [1]	Relatively inexpensive equipment. Less complex algorithm	Designed for wafer. No absolute height. Assumes ball peaks in a plane.
Moiré projection method [2]	Accurate height. Automated algorithm	Complex setup and algorithm. Expensive equipment. Long measurement time.
Con-focal tool	Accurate height. Automated algorithm	Complex setup and algorithm. Expensive equipment. Long measurement time.

Automated ball height algorithm with less complex setup and computation is needed.

Imaging Setup and Camera Calibration

Stereo Imaging Setup
- Two area-scan cameras
- Same camera angle from opposite sides
- Ring lights at the same opposite angle w.r.t cameras

Camera Calibration
- Calculate camera parameter and relative poses of two cameras.
- Using a planar calibration pattern and the MATLAB Camera Calibration Toolbox [3]
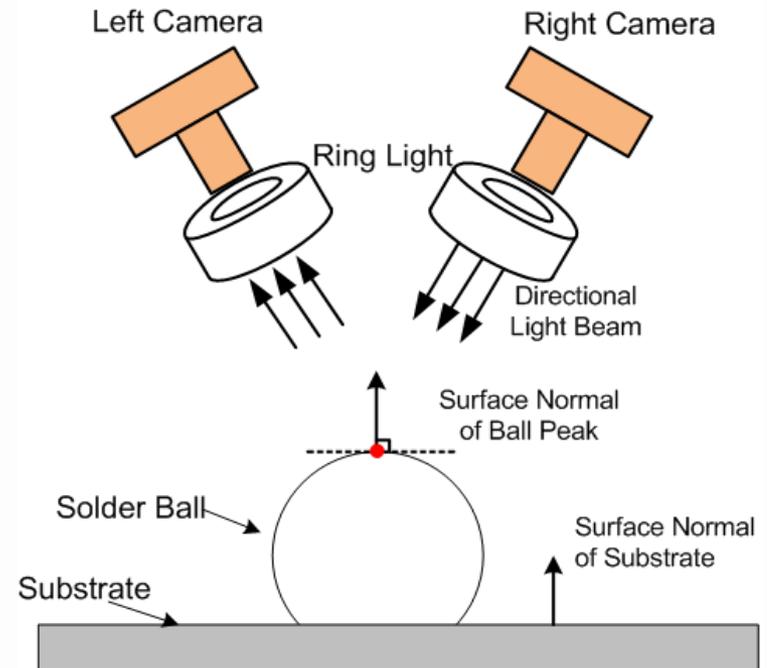
❑ **Imaging Setup uses stereo cameras and ring lights.**
❑ **Calibration uses images of planar patterns.**

Automated Solder Ball Height Detection Method
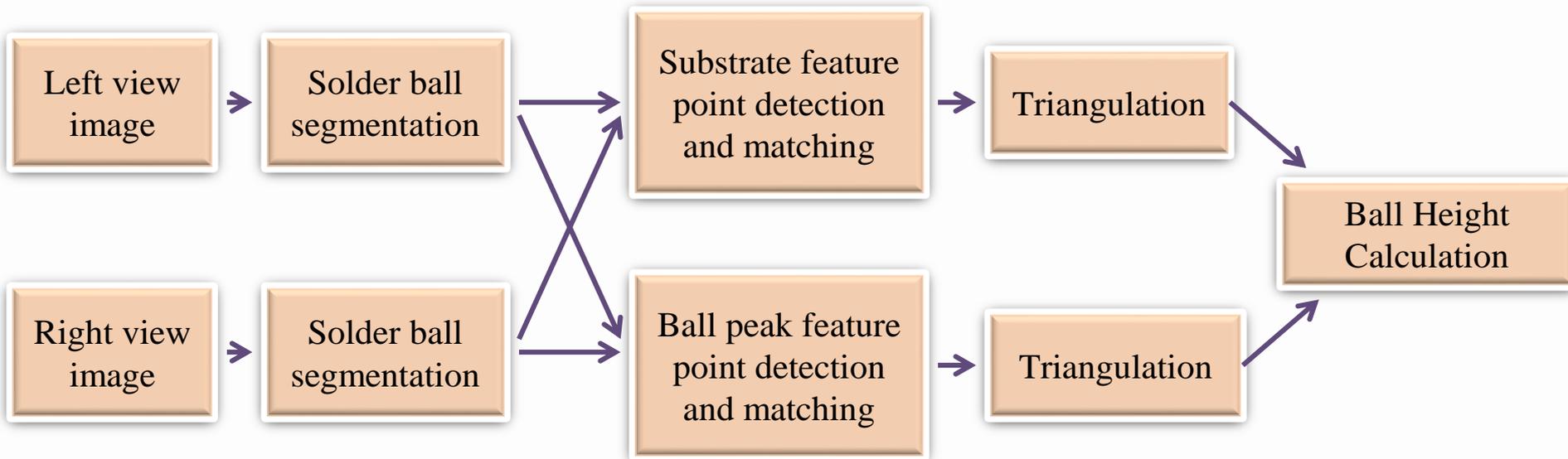
Automated Solder Ball Height Detection Method
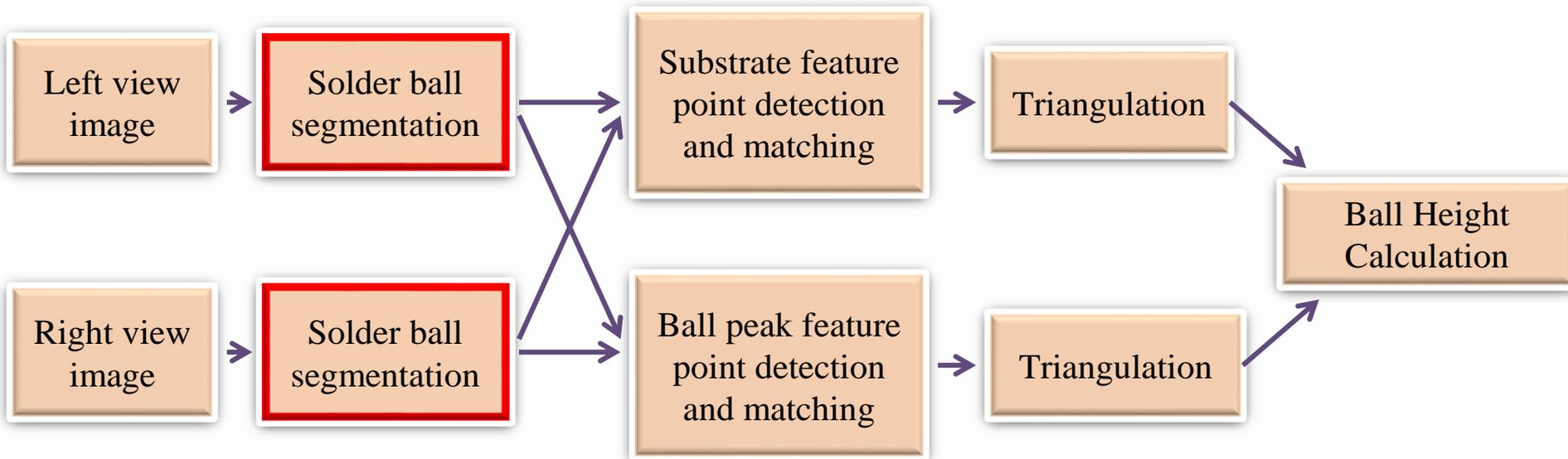
Solder Ball Segmentation
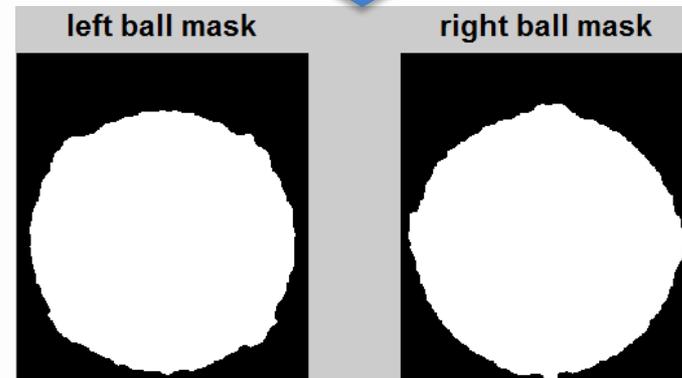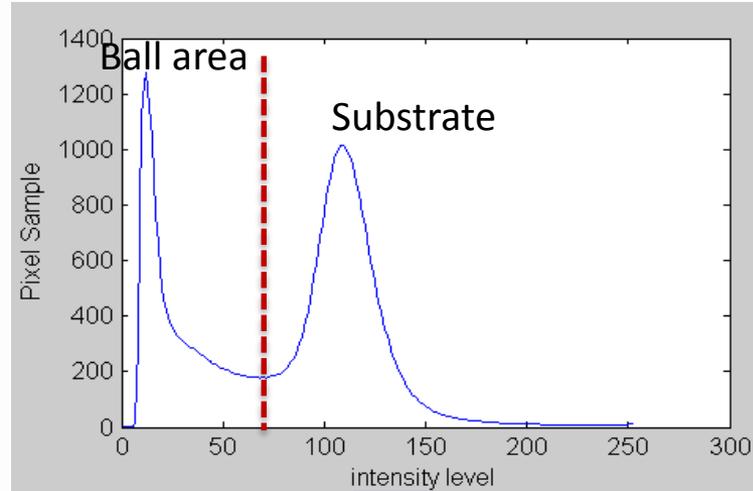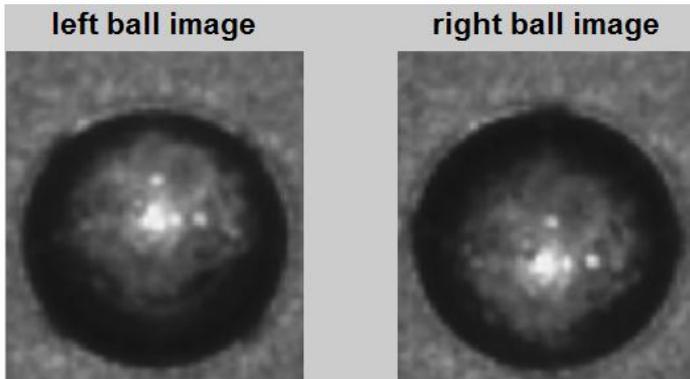
Segmentation:
- find threshold using an adaptive thresholding method based on histogram analysis [4]
- morphological opening operations
- Circle fitting

Thresholding segmentation gives accurate ball masks.

Automated Solder Ball Height Detection Method
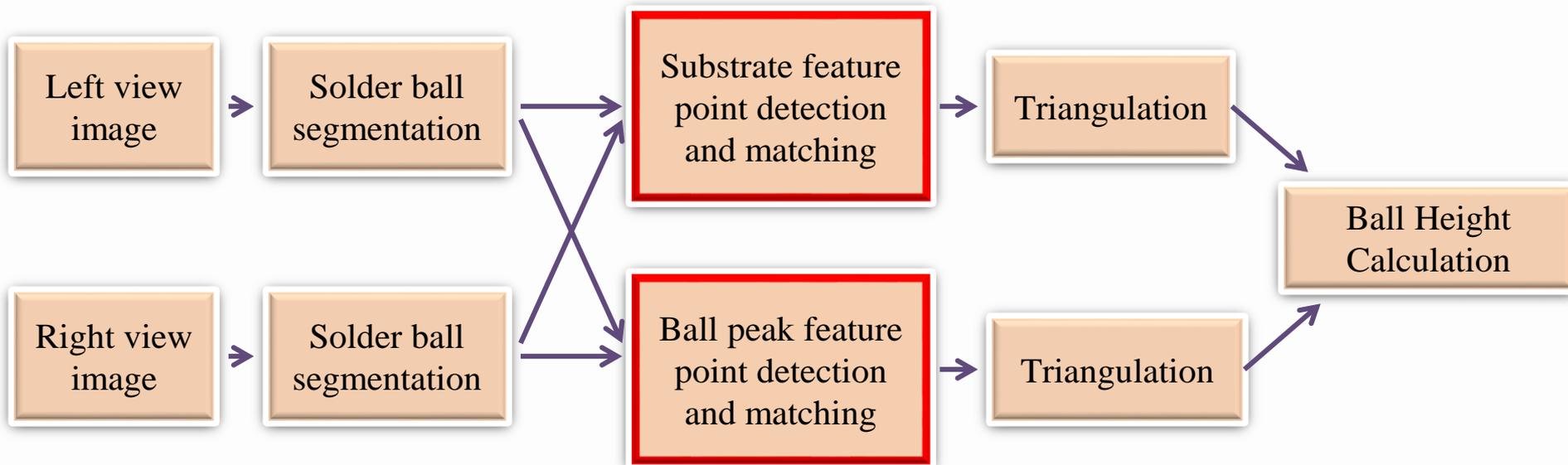
# Substrate Feature Point Detection

Matching substrate Feature Points:

Centroid points of corresponding ball mask in left image and right image.
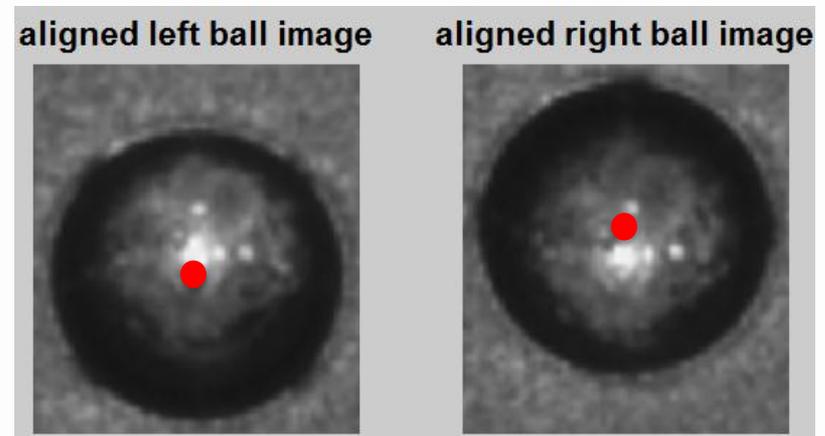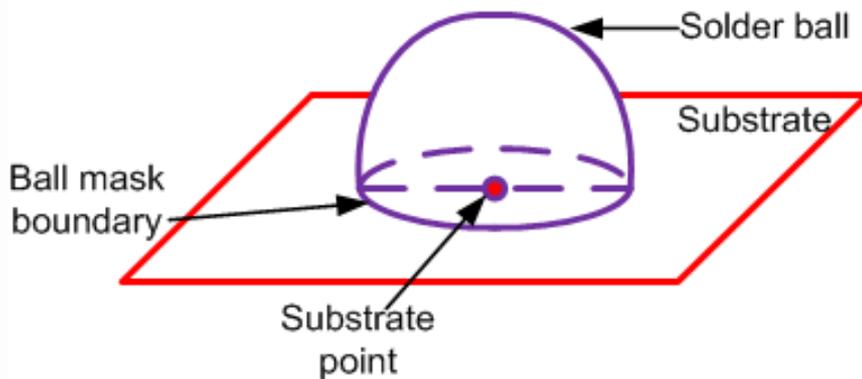
Substrate features are calculated from ball mask.

Ball Peak Feature Point Detection

aligned left ball image

aligned right ball image

left ball peak image

right ball peak image
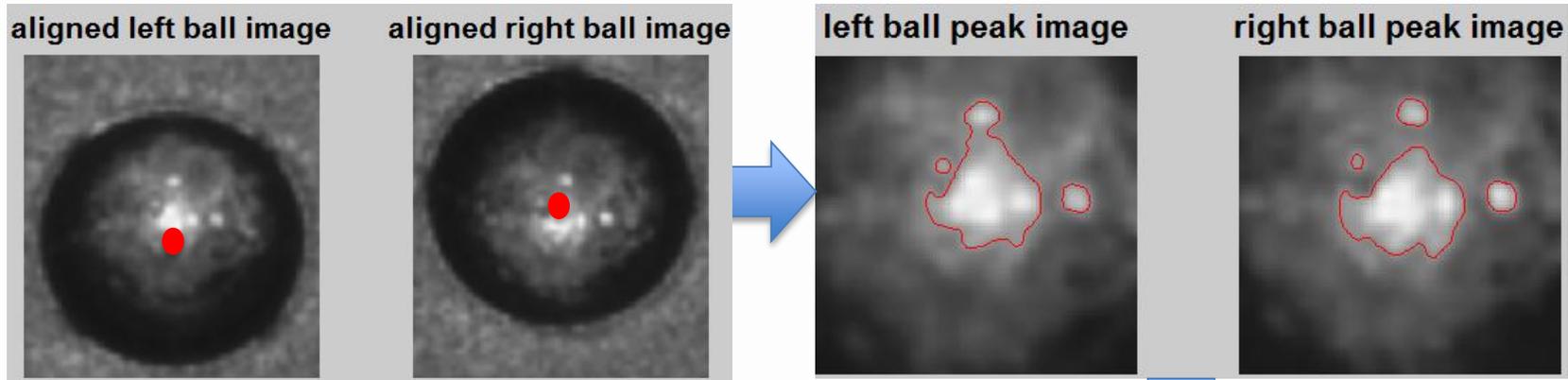
Matching Feature Points:
centroid of each matching region
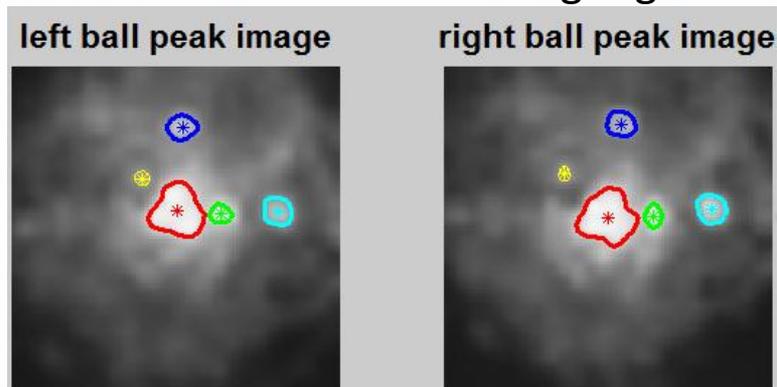
Multiple iso-contours:
tree graph matching

left ball peak image

right ball peak image

iso-contour map of left view

iso-contour map of right view
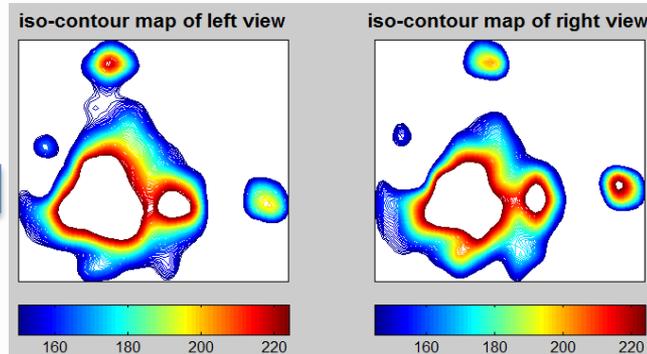
iso-contour: the curve with the same intensities

Ball peak features are detected using iso-contour structures in images

APEX EXPO IPC

MARCH 25-27, 2014
MANDALAY BAY RESORT AND
CONVENTION CENTER
LAS VEGAS, NEVADA

NEW IDEAS ... FOR NEW HORIZONS

Automated Solder Ball Height Detection Method
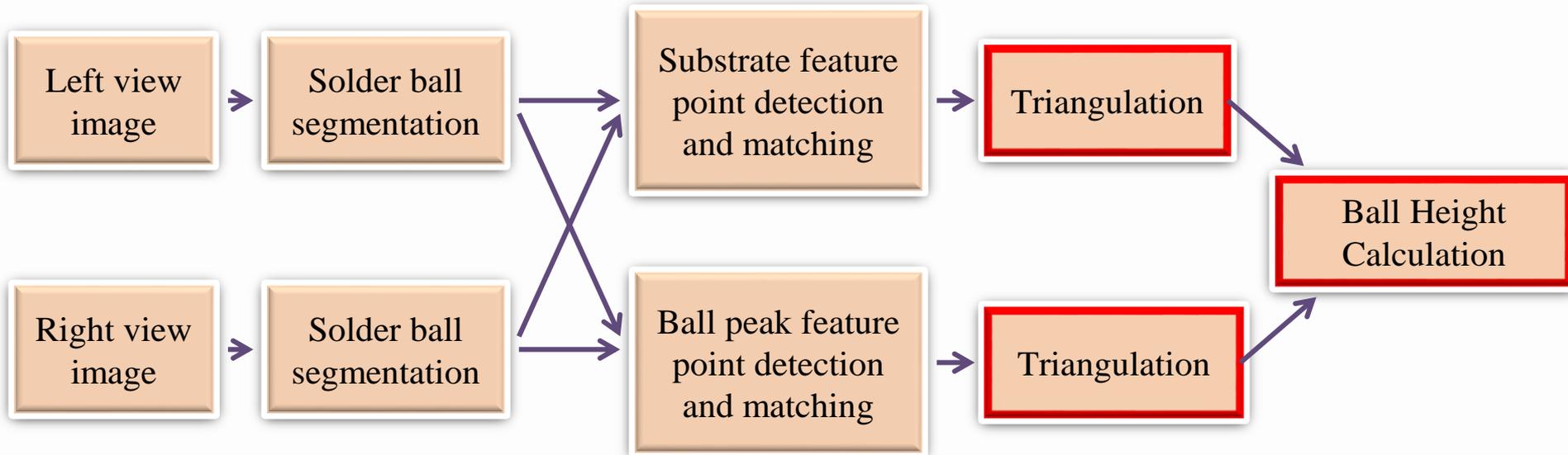
# Triangulation and Ball Height Calculation

- Triangulation [5] of corresponding 2D points generates 3D coordinates of feature points
- Ball Height = Euclidean distance between 3D substrate point and 3D ball peak point
- For multiple 3D ball peak points, choose the highest ball height value.

left ball peak image

right ball peak image

Ball peak 2D feature points

3D Substrate Point   3D Ball Peak Point

Left image

Right image

Left camera

Right camera

Ball peak 3D points

Z-axis

Ball Height

Substrate 3D point

Y-axis

X-axis
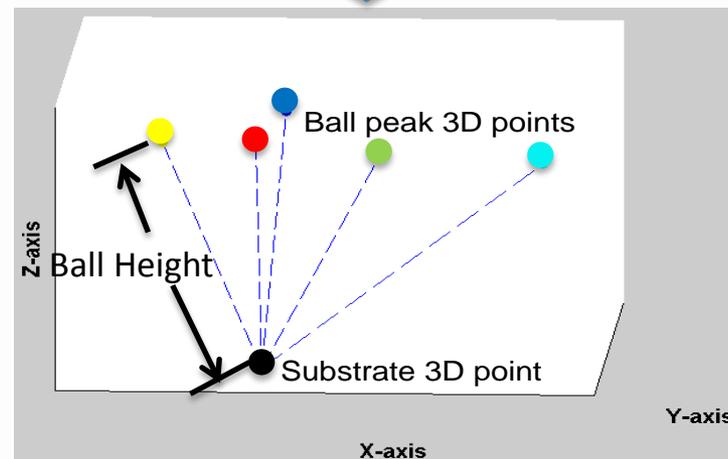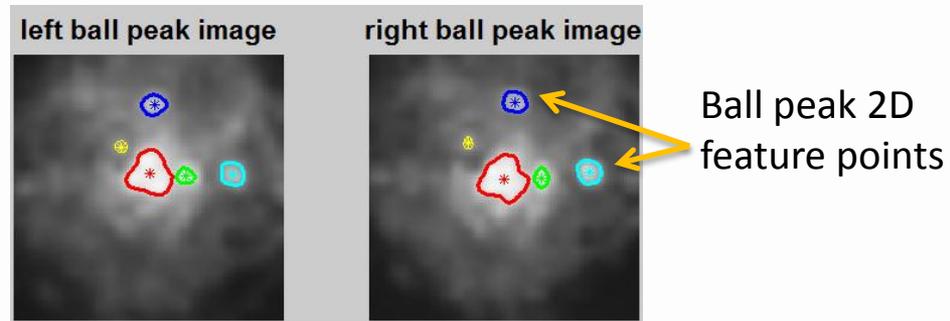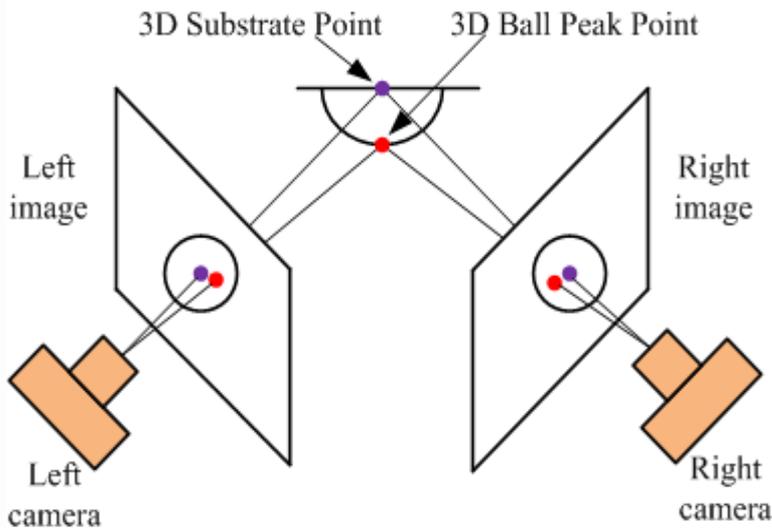
Triangulation calculated the 3D points for both substrate and ball peak

# Experimental Results – Ball Height 1

Ball Height of 76 balls on a package, compared with con-focal camera tool height results.


Ball Height: Calculated vs. Ground-truth
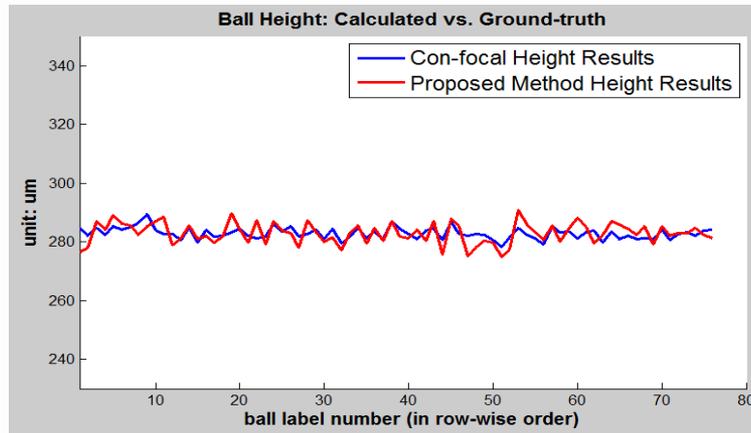
Mean Squared Error on 3 products

Package	No. of Balls Tested	Avg. Ball Height
Product A	76	281.5 um
Product B	151	282.1 um
Product C	156	382 um

APEX EXPO
IPC

NEW IDEAS ... FOR NEW HORIZONS

MARCH 25-27, 2014
MANDALAY BAY RESORT AND CONVENTION CENTER
LAS VEGAS, NEVADA
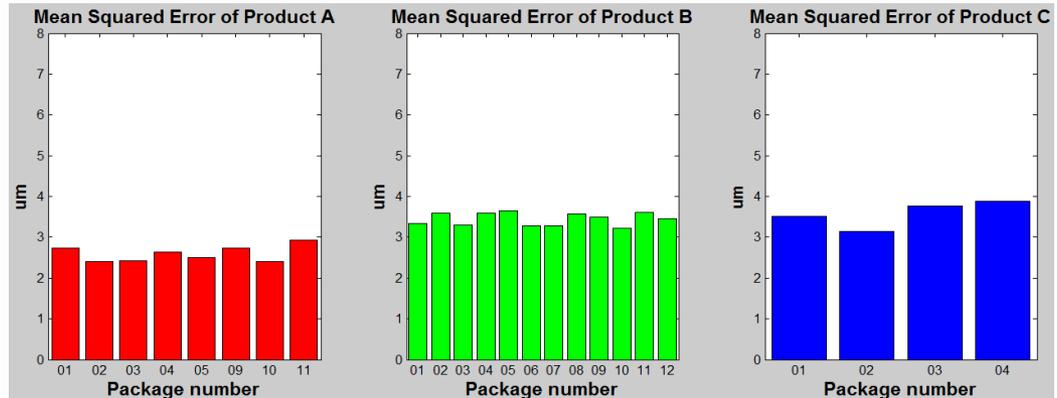
Experimental Results – Ball Height 2

Ball Height of 17 balls on a package, compared with laser profiling height results.

Accuracy is .8853 correlation squared (>.75 is matching)

Correlation Analysis
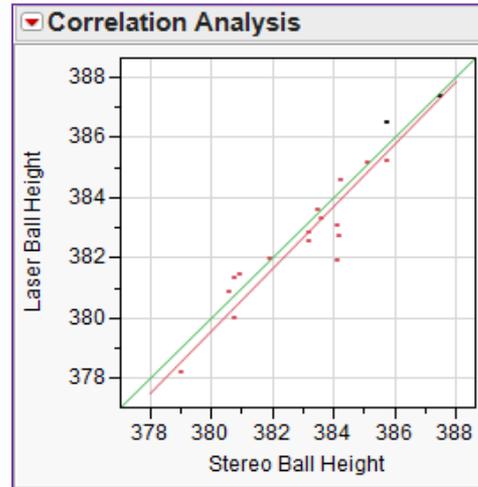
P/T ratio is 7.9% (repeatability <20% is considered capable)

Variability Chart for Solder Ball Height

* Stereo Vision Method
○ Confocal Camera Tool
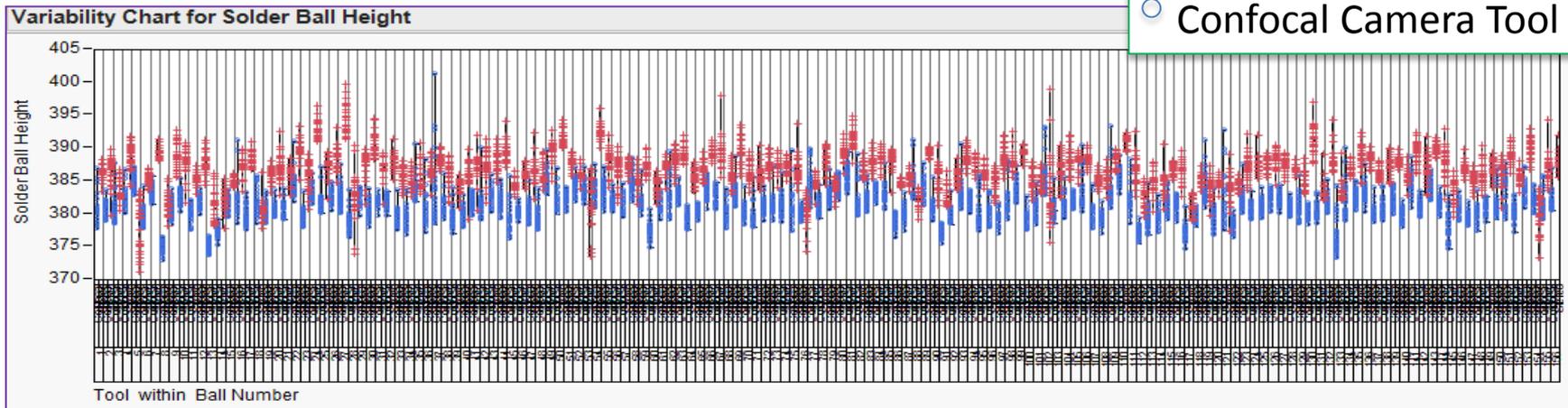
**Accuracy and repeatability prove the capability of the method.**

Experimental Results – Warpage 1

Coplanarity can be represented using the depth values of substrate points.
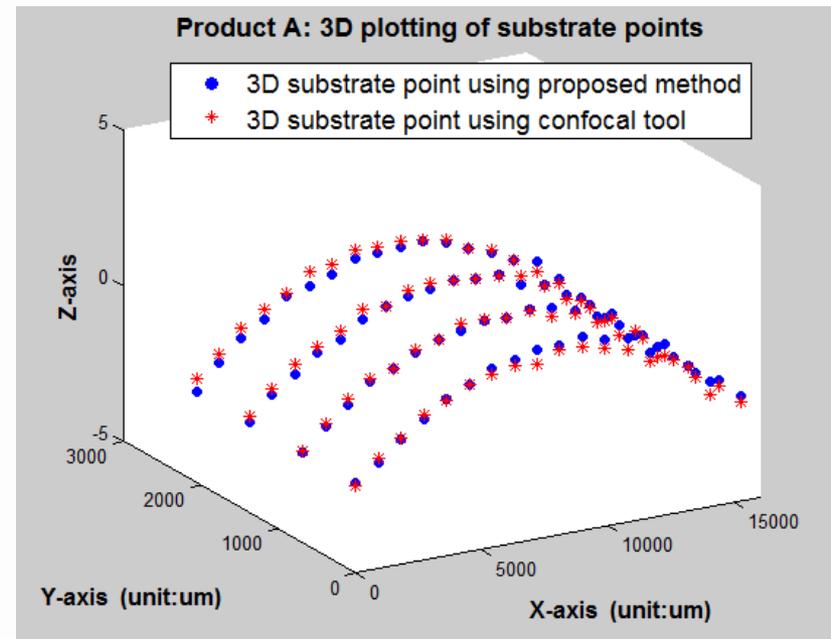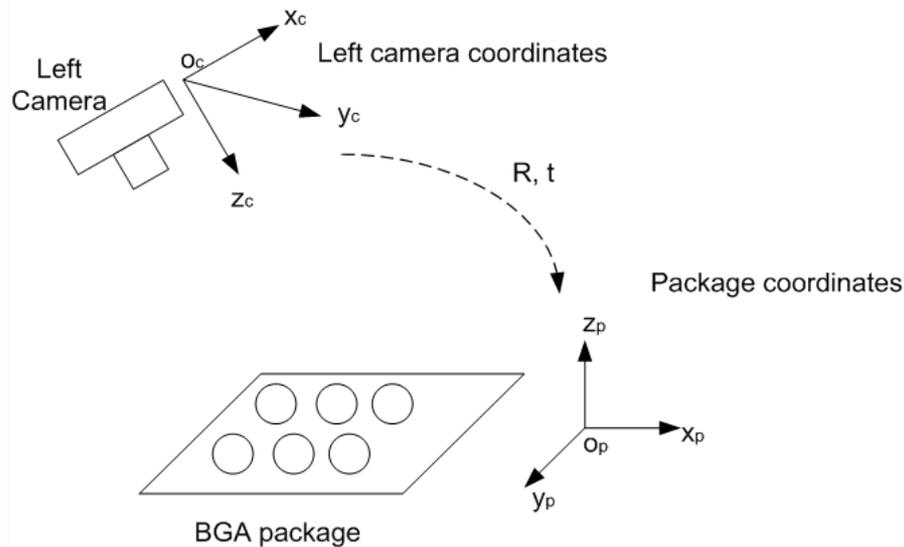
Experimental Results – Warpage 2

Accuracy is .97 correlation squared (>.75 is matching)
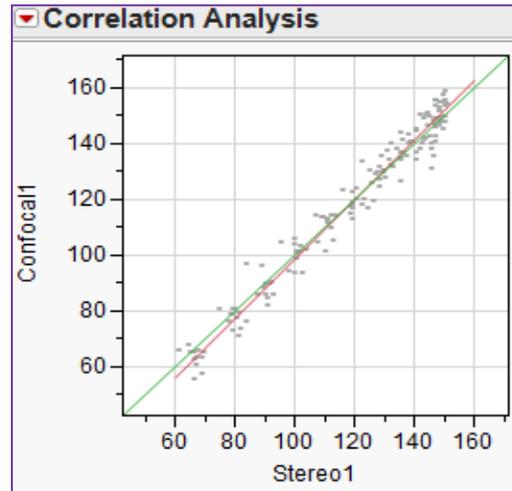
P/T ratio is 3.0% (repeatability <20% is considered capable)

Correlation Analysis

* Stereo Vision Method
○ Confocal Camera Tool

Variability Chart for Coplanarity
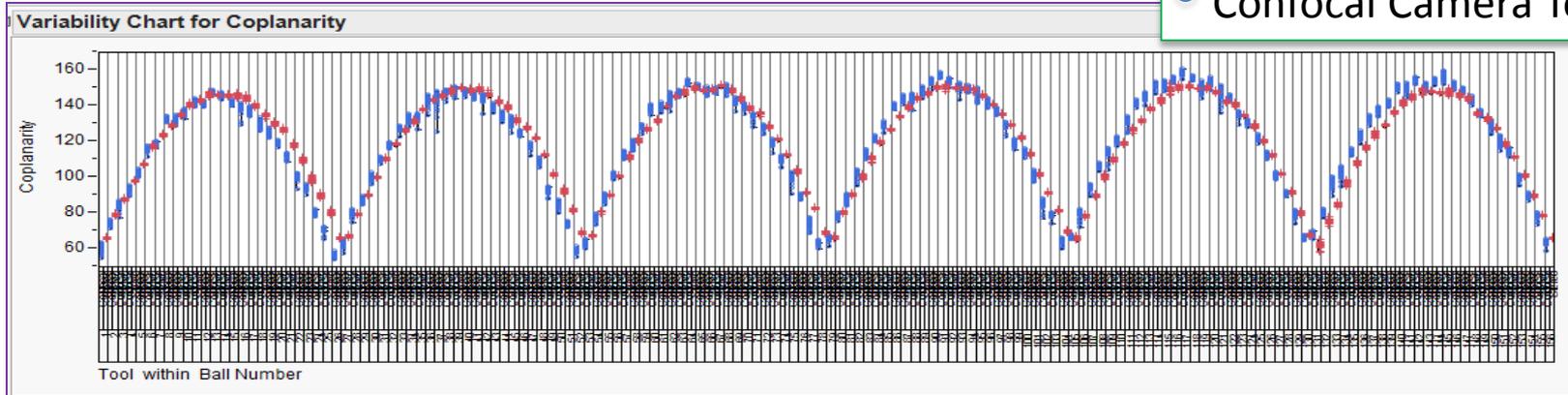
Accuracy and repeatability prove the capability of the method.

Summary

- The algorithm provides reliable, accurate ball height detection automatically from stereo images.

- The algorithm provides reliable, accurate warpage results.

- The algorithm operates automatically without any operator intervention.

- The statistics show that the algorithm performs comparably with con-focal tools.

- The algorithm is easy to implement and can save setup cost and computation time.

References

[1] M.Dong, R.Chung, Y.Zhao and E.Y. Lam, "Height Inspection of Wafer Bumps Without Explicit 3D Reconstruction," Proceedings of SPIE the International Society for Optical Engineering, vol. 6070, pp. 607004, 2006.

[2] H. Ding, R. E. Powell, C. R. Hanna and I. C. Ume, "Warpage Measurement Comparison Using Shadow Moiré and Projection Moiré Methods," IEEE Transactions on Components and Packaging Technologies, vol. 25, no. 4, 2002.

[3] Camera Calibration Toolbox for Matlab Website:
http://www.vision.caltech.edu/bouguetj/calib_doc/index.html#ref

[4] A. F. Said, B. L. Bennett, L. J. Karam and J. S. Pettinato, "Automated Detection and Classification of Non-wet Solder Joints," IEEE Transactions on Automation Science and Engineering, vol. 8, no. 1, 2011.

[5] R. Hartley and A. Zisserman, "Multiple View Geometry in Computer Vision," Cambridge University Press, 2002.